



Expanded CUG Repeats Trigger Disease Phenotype and Expression Changes through the RNAi Machinery in *C. elegans*

Lena Qawasmi^{1,†}, Maya Braun^{1,†}, Irene Guberman¹, Emiliano Cohen¹, Lamis Naddaf¹, Anna Mellul¹, Olli Matilainen², Noa Roitenberg³, Danielle Share¹, Doron Stupp¹, Haya Chahine¹, Ehud Cohen³, Susana M.D.A. Garcia², and Yuval Tabach¹

1 - Department of Developmental Biology and Cancer Research, Institute for Medical Research Israel-Canada (IMRIC), Faculty of Medicine, The Hebrew University of Jerusalem, Ein Kerem, Jerusalem, Israel

2 - Institute of Biotechnology and HiLIFE, University of Helsinki, Helsinki, Finland

3 - Department of Biochemistry and Molecular Biology, Institute for Medical Research Israel-Canada (IMRIC), Faculty of Medicine, The Hebrew University of Jerusalem, Ein Kerem, Jerusalem, Israel

Correspondence to Susana M.D.A. Garcia and Yuval Tabach: susanamaria.garcia@helsinki.fi, yuvaltab@ekmd.huji.ac.il
<https://doi.org/10.1016/j.jmb.2019.03.003>

Edited by Sybille Krauss

Abstract

Myotonic dystrophy type 1 is an autosomal-dominant inherited disorder caused by the expansion of CTG repeats in the 3' untranslated region of the DMPK gene. The RNAs bearing these expanded repeats have a range of toxic effects. Here we provide evidence from a *Caenorhabditis elegans* myotonic dystrophy type 1 model that the RNA interference (RNAi) machinery plays a key role in causing RNA toxicity and disease phenotypes. We show that the expanded repeats systematically affect a range of endogenous genes bearing short non-pathogenic repeats and that this mechanism is dependent on the small RNA pathway. Conversely, by perturbing the RNA interference machinery, we reversed the RNA toxicity effect and reduced the disease pathogenesis. Our results unveil a role for RNA repeats as templates (based on sequence homology) for moderate but constant gene silencing. Such a silencing effect affects the cell steady state over time, with diverse impacts depending on tissue, developmental stage, and the type of repeat. Importantly, such a mechanism may be common among repeats and similar in human cells with different expanded repeat diseases.

© 2019 Elsevier Ltd. All rights reserved.

Introduction

DNA repeats are patterns of one or several nucleic acids that occur in multiple copies throughout the genome. Beyond a certain copy number threshold, repeats are unstable and tend to expand. This can occur during meiosis over generations or in the same individual during replication, recombination, or mismatch repair. Expansions of DNA repeat sequences, mostly trinucleotide repeats, are associated with over 30 human genetic diseases such as fragile X syndrome, myotonic dystrophy types 1 and 2 (DM1, DM2, respectively), and Huntington's disease [1].

Expansion of a non-coding trinucleotide repeat sequence can be toxic to the cell, causing human pathogenesis through trans-acting dominant mechanisms. Toxic RNAs are expressed ubiquitously, yet

repeat-based disorders are often neuro-muscular, exhibiting various degenerative and progressive symptoms. The age of onset, severity of symptoms, and pace of disease progression often show a tight correlation with the repeat length. It is enticing to consider that the similarities shared by these disorders stem from a common pathogenic mechanism and that standard therapeutic approaches could address phenotypes associated with currently incurable conditions.

DM1 is an autosomal-dominant neurodegenerative disease whose patients present a range of symptoms characterized by progressive muscle wasting, atrophy, and myotonia [2]. DM1 results from an unstable expansion of a CTG trinucleotide repeat in the 3' untranslated region (3'UTR) of a serine-threonine protein kinase (DMPK) gene. In healthy individuals, the DMPK gene contains 5–37 CTG repeats.

Individuals who carry 38 to 49 CTG repeats are asymptomatic but considered as carrying pre-mutation alleles. In DM1 patients, the repeat length ranges from 50 to 4000 [3].

RNAs bearing expanded repeats form stable hairpins, which accumulate as RNA foci in the nucleus [4]

and abnormally interact with double-stranded RNA (dsRNA)-binding proteins. The aberrant RNAs are suggested to disrupt several cellular processes, affecting cellular function and resulting in toxicity. Several mechanisms have been suggested to explain the toxic phenotypes in DM1 including RNA gain of

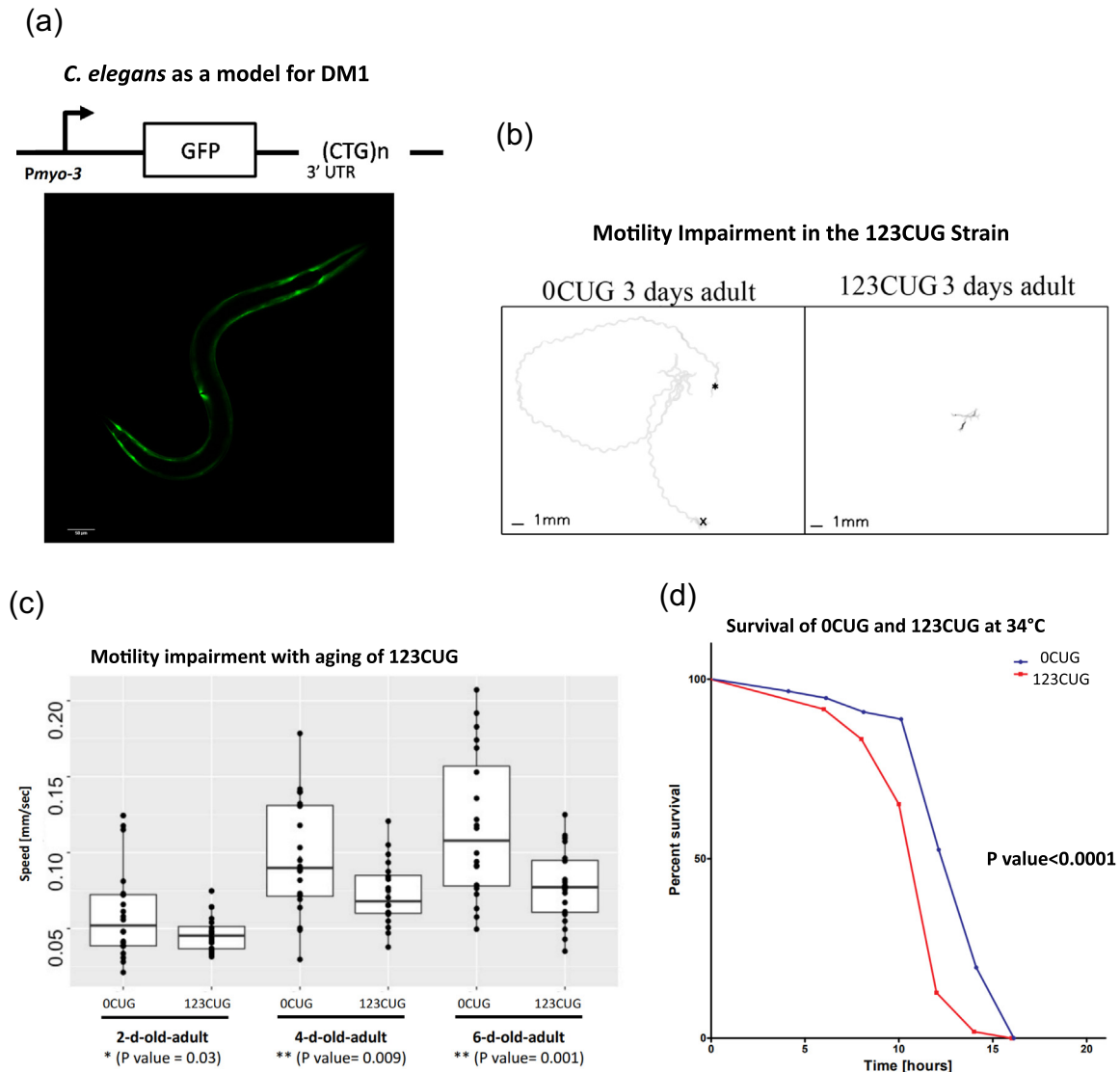


Fig. 1. *C. elegans* model for DM1. (a) Schematic outline of the CUG repeat-bearing constructs stably inserted into N2 animals. *C. elegans* expresses GFP under a body-wall muscle-specific promoter, the *myo-3* promoter (*myo-3p*). (b) Motility impairment in the 123CUG strain. Micrograph example illustrating tracks left by 3-day-old 123CUG and 0CUG animals 5 min after being placed at the position marked by the asterisk. Experiments were performed at room temperature, and “x” indicates the animals' position at the end of 5 min. (c) Motility impairment with aging of 123CUG. Analysis of 123CUG motility impairment. Box-dot plot corresponds to 123CUG and 0CUG animal speed. A significant difference was observed in the speed of all different life stages of 123CUG adults as compared to 0CUG controls (* $P < 0.05$, ** $P < 0.001$, *t* test). Twenty animals were analyzed for each strain at room temperature. Three independent experiments were performed. (d) Survival of 0CUG and 123CUG at 34 °C. Survival under heat stress conditions (34 °C) was impaired in 1-day-adult 123CUG animals as compared to 1-day-adult 0CUG ($n = 60$, $P < 0.0001$). (e) Relative gene expression before and after heat shock. qPCR of heat shock protein genes before and after exposure to 8 h at 34 °C heat stress. Expression is relative to wild-type N2 worms maintained in normal conditions. mRNA levels of heat shock protein genes *hsp-16.2* and *hsp-70* increase after an 8 h exposure to heat stress in 1-day-adult 0CUG and 123CUG animals. Two biological replicates, with three technical replicates each, were analyzed in this experiment. HS, heat shock.

(e)

Relative gene expression before and after heat shock

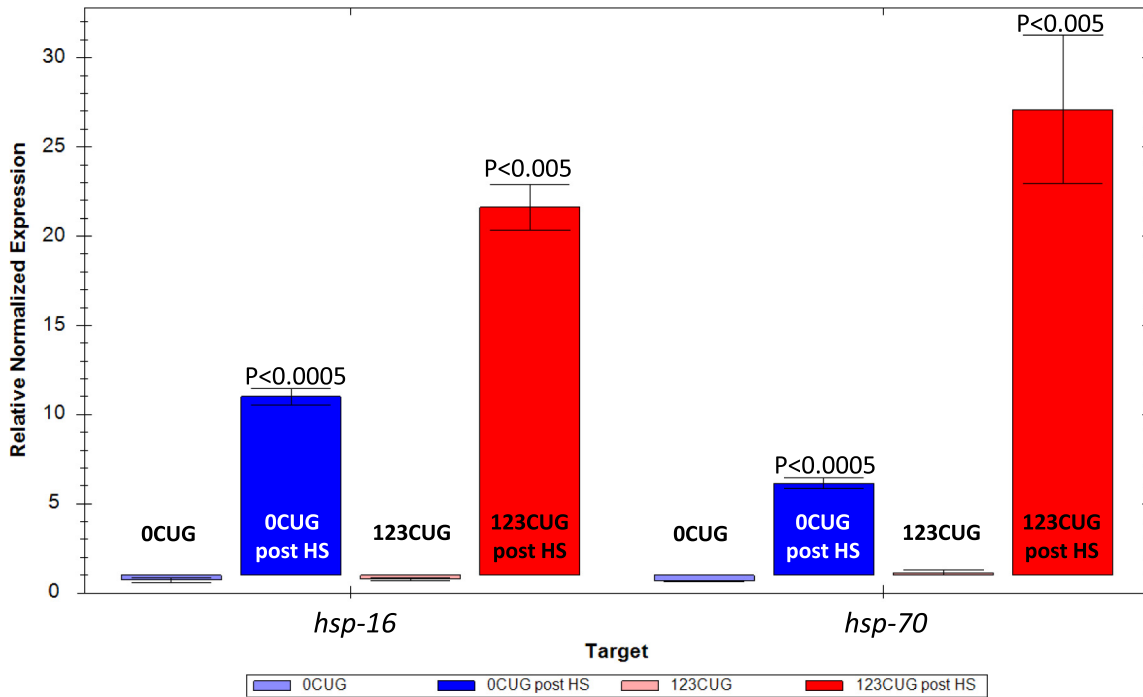


Fig. 1. (continued).

function [5], protein sequestration [6], repeat associated non-ATG translation [7], microRNA dysregulation [8], and involvement of the RNA interference (RNAi) machinery [9].

Only a few DM modifiers of toxicity have been identified and a handful have been characterized. These include the alternative splicing factors muscleblind-like 1 (MBNL1) and CUG binding protein 1 (CUGBP1), which are disrupted by expanded RNA repeats and contribute to DM pathogenesis [6]. MBNL1 is sequestered by the CUG foci and its depletion from the nucleoplasm results in loss of function and deregulation of its various targets, including transitions from an adult to embryonic splicing patterns in striated muscle [4,6]. Furthermore, MBNL1 has a significant role in the regulation of different RNA processes, including the biogenesis of miRNAs. Accordingly, changes in miRNA expression and cellular distribution have been found in DM1 skeletal muscle [10], with multiple miRNAs downregulated in muscle biopsies. As a result, several of their downstream targets were upregulated [8]. Thus MBNL1 sequestration may be accountable for miRNA dysregulation in DM1 muscle biopsies [11]. Nevertheless, although MBNL1 knockout mouse models recapitulate the muscle pathology observed in DM1 skeletal muscle [12], they do not reproduce all DM1 phenotypes [13,14]. In addition, MBNL1 overexpression in CUG repeat-expressing

human cell lines does not completely rescue the pathogenesis. These observations further support the notion that additional mechanisms, beyond MBNL-dependent pathways, contribute to DM1 pathogenesis [15].

Overall, the underlying pathogenic mechanisms of RNA toxicity in DM1 are not fully understood. Still, expanded repeat RNAs are known to disrupt of RNA binding proteins and splicing factors. Thus, it is reasonable to propose that the RNAi machinery (that targets RNA) may also interact and be affected by expanded repeats. RNAi is involved in diverse biological processes including transcriptional gene silencing, post-transcriptional regulation, and antiviral responses.

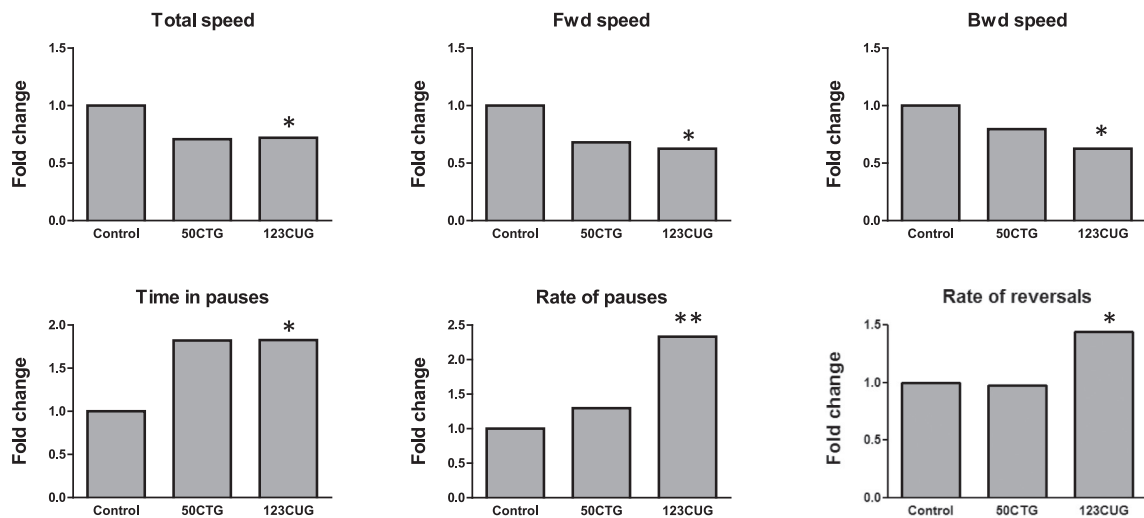
Expanded RNA repeats form stable hairpin structures and these dsRNA strands are known to serve as a substrate for the nuclease Dicer [16]. Recent studies have shown that although Dicer is normally active in the cytoplasm, it can enter the nucleus and gain access to the DM1 RNA expanded repeat [17]. These RNAs molecules could then be cleaved to short CUG repeats, which act as siRNA and activate the RNAi silencing pathway [16]. RNA repeats also generate anti-sense transcripts, which together with the sense transcript may constitute an additional Dicer substrate as they accumulate as foci in the nucleus. Anti-sense foci have been described in many trinucleotide repeat

diseases including DM1 [18]. This mechanism of Dicer activity can attenuate the expression of the mutant sequence and may have additional effects. Dicer also has a global regulatory activity; thus, any disruption of Dicer's normal activity has the potential to affect different genes and pathways.

To study the possible crosstalk between RNAi and RNA toxicity, we further developed a characterized set of *Caenorhabditis elegans* models for DM1 [4]. Muscle proteins are highly conserved among species, and the nematode *C. elegans* has emerged as a preferred model organism for the study of neuromuscular

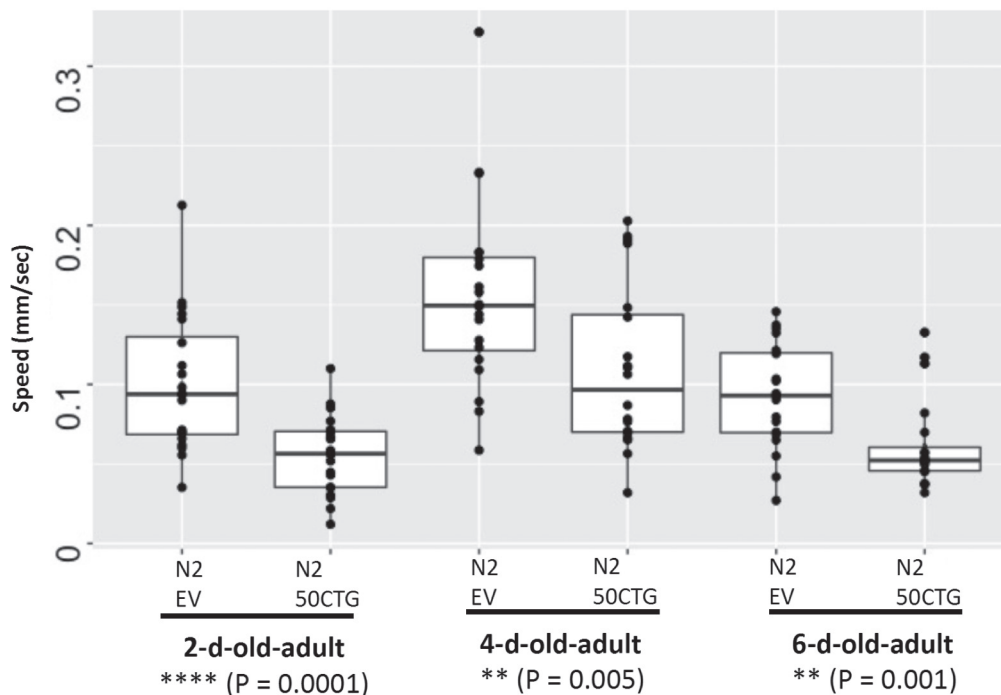
(a)

N2 50CTG RNAi motility mimics 123CUG



(b)

Motility impairment with aging of N2 50CTG RNAi



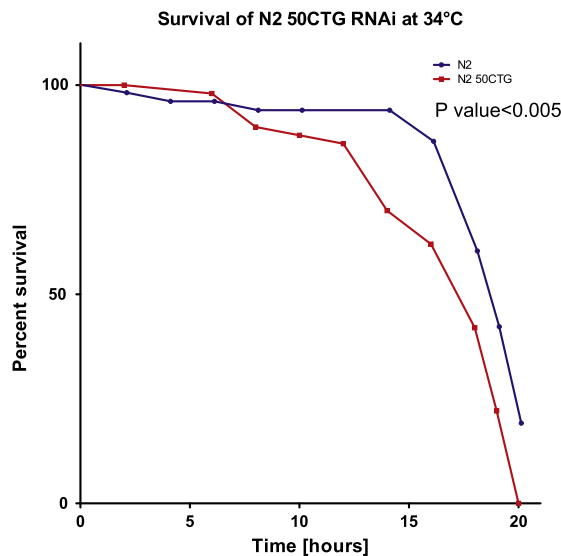


Fig. 2. RNAi of 50CTG mimics phenotypes seen in 123CUG animals. (a) N2 50CTG RNAi motility mimics 123CUG. Locomotion patterns for 3-day-old adult N2 animal fed 50CTG RNAi are similar to 123CUG when each is compared to its control (N2 with EV bacteria and 123CUG to 0CUG, respectively). Data were obtained from two independent experiments. In each experiment, five animals were analyzed. The P value was not significant for 50CTG RNAi, but the trend was similar to the significant value observed in 123CUG animals ($*P < 0.05$, $**P < 0.01$). (b) Motility impairment with aging of N2 50CTG RNAi. 50CTG RNAi feeding causes motility impairment. Box-dot plot identifies the speed of N2 fed with 50CTG RNAi as compared with N2 fed EV. Motility was analyzed for 20 animals of each strain at room temperature at three different ages: 2-, 4-, and 6-day-old adults. A significant decrease in 50CTG-fed animal's speed was observed relative to EV-fed animals. Three biological repeats were performed for each strain ($****P < 0.0001$, $**P < 0.01$). (c) Survival of N2 50CTG RNAi at 34 °C. Survival curve under heat shock conditions (34 °C). The 50 CTG RNAi significantly reduced the worm's life span ($n = 60$, $P < 0.005$).

degenerative disorders. Available nematode-based methods enable a careful characterization of locomotion, muscle structure analysis, and pathology identification nominating this animal as an excellent model in muscular dystrophy studies. In addition, *C. elegans* has a robust RNAi system, including a highly conserved Dicer that contains all the major functional domains of human Dicer [17]. The DM1 *C. elegans* model used here has an integrated transgene bearing a green fluorescent protein (GFP) gene with a 3'UTR CTG repeat of different lengths. These animals express the transcripts in their body wall muscle cells and recapitulate DM1 phenotypes, such as loss of muscle function and nuclear foci accumulation [6]. The phenotypes exhibited by these strains allow us to look directly at the effects of RNA toxicity on cell and tissue dysfunction.

Here we studied the role of the RNAi machinery in the pathogenicity of microsatellite expansion disorders. Our results show a tight association between the RNAi machinery, RNA toxicity, and DM1 disease phenotypes in worms. These associations can explain some of the complex phenotypes observed in DM1, and possibly in other diseases, and point at novel research avenues for the development of new remedies for DM1.

Results

Expanded CUG repeat expression causes *C. elegans* muscle dysfunction

The *C. elegans* DM1 model used in this study expresses 123 CUG repeats (123CUG, strain GR2024) in the 3'UTR of a GFP under the *myo-3* body wall muscle-specific promoter [4] (Fig. 1a), whereas the control strain contains no repeats (0CUG, strain GR2025). Initially, we aimed to characterize the pathogenicity of these repeats by establishing the DM1's motility defect. The 123CUG animals showed impaired motility as compared to 0CUG animals. They exhibited a slower crawling speed, covering shorter distances as reflected by the individual worm tracks [19] (Fig. 1b). A population of 123CUG and 0CUG animals at different ages (2-, 4-, and 6-day-old adults) were analyzed by a multi-tracking software. The results showed that not only did 123CUG animals move slower than 0CUG, but also their motility defect worsened with age relative to controls (Fig. 1c). Next, we examined whether the toxic RNAs increased susceptibility to stress in our animals. To test this, 60 animals from each strain were exposed to heat shock (34 °C) at their first day of adulthood. Living animals were scored in 2-h intervals. 123CUG animals exhibited an increased sensitivity to heat stress (Fig. 1d). After 15 h of exposure, approximately 75% of the 0CUG worms were alive compared to merely 25% of their counterparts that had expressed the 123CUG construct.

To assess the animals' ability to activate the heat shock response and to test whether the 123CUG susceptibility to stress stems from its inability to mount a proper response, we used qPCR to measure the levels of two heat-responsive genes: *hsp-16.2* and *hsp-70* in 1-day-old adult 0CUG and 123CUG strains before and after 8 h of exposure to heat. *hsp-70* is a member of the conserved Hsp70 family of large ATP-dependent molecular chaperones. *hsp-16.2* is an ortholog of human HSPB1 [heat shock protein family B (small) member 1]. The gene expression was adjusted to an age-matched control group of N2 worms. As depicted in Fig. 1e, *hsp-70* levels increased over 6-fold in 0CUG worms and 27-fold in 123CUG worms following exposure to 8 h of heat shock. *hsp-16.2* levels increased 11-fold and 21-fold in 0CUG and 123CUG

animals, respectively. These results indicate that the heat shock response is not only conserved in 123CUG worms but even hyper-activated. Namely, activation of the heat shock genes tested is not disrupted by the presence of CUG repeats. Our data support a model in which the reduced survival caused by heat stress in DM1 animals is the likely result of a complex disease dysfunction rather than the organism's inability to activate heat shock proteins [20].

Feeding *C. elegans* with CTG dsRNA mimics effects seen in 123CUG animals

Expanded RNA repeats can be processed to short CUG repeats, which act as siRNAs and can be used in the RNAi silencing pathway [16]. To evaluate the potential phenotypic effects of the CUG repeats and its contribution to the disruption of cellular processes, we fed wild-type (N2) animals with bacteria that harbor plasmids (L4440) expressing RNAs bearing 50CTG repeats (50CTG RNAi). Normally, exogenous dsRNA taken up by feeding triggers the RNAi machinery and causes gene silencing. This direct activation of the RNAi pathway separates the phenotypic effects caused by the RNAi pathway from other potential confounders of toxicity (i.e., sequestering of proteins). We tested the effects of 50CTG RNAi on the motility of 3-day-old adult worms using a single-worm tracker assay. 50CTG RNAi animals exhibited slower locomotion, including both forward and backward movements, and paused more often and for longer periods relative to N2 controls fed empty vector (EV) bacteria (Fig. 2a). In addition, we analyzed these animals' motility using a multi-tracking assay at different ages during adulthood. Twenty animals were tested on their second, fourth, and sixth days of adulthood at room temperature. The results showed a significant reduction in crawling speed of N2 animals that were fed with 50CTG RNAi as compared to N2 animals fed with the EV bacteria, at all three ages tested (Fig. 2b). The speed of 6-day-old adult N2 animals fed 50CTG RNAi (at an average of 0.061 mm/s) was reduced relative to N2 animals fed EV with velocities of 0.092 mm/s. Moreover, 1-day-old adult animals fed 50CTG RNAi exhibited a small, yet significantly shorter survival time (Fig. 2c) following heat stress. The effect was weaker than the 123CUG animals (Fig. 1d). Together these data suggest that the RNAi machinery, through a potential broadening of its "effects," contributes to DM disease phenotypes. Overall, these data support a moderate but meaningful role for the small RNA pathways in DM pathogenesis.

Downregulation of RNAi genes rescues GFP expression levels of 123CUG animals

One of the interesting phenotypes described for 123CUG strains [4] is the drastic decrease in GFP protein levels as animals reach adulthood. We observed that 3-day-old 123CUG adults exhibited approximately an 88% reduction of the GFP signal detected relative to L2 123CUG animals, whereas 0CUG showed only a mild decrease (Fig. 3). Recently, it was shown that the nonsense-mediated mRNA decay pathway contributes to expanded RNA clearance [4] and therefore leads to reduction in GFP levels. However, we hypothesized that the strong reduction in GFP levels observed in adult 123CUG animals also resulted from the 123CUG RNAs serving as a template and self-targets to the RNAi machinery. To test this and determine which factors in the RNAi machinery (if any) affect the GFP reduction observed in 123CUG animals, we used RNAi to screen 50 genes known to participate in gene silencing through the RNAi pathway (Table 1). We visually compared the GFP signal of 3-day-old 123CUG adults fed control bacteria (EV) to animals that had different RNAi genes downregulated. Silencing of specific factors in the RNA machinery (using the RNAi machinery) is a common practice [21,22] that causes a reduction in the transcription level. GFP brightness was determined for the entire plate by scoring each plate separately using a Nikon C2 confocal microscope and by complementary examination of specific worms using confocal microscopy as shown in Fig. 1S and Table 1. Of the 50 genes tested, 22 were positive, of which 7 showed strong rescue (a mild decrease in GFP fluorescence in comparison to 123CUG animals grown on control bacteria). The remaining genes analyzed were negative (24 genes) or their knockdown (4 genes) showed deleterious effects on development and/or growth.

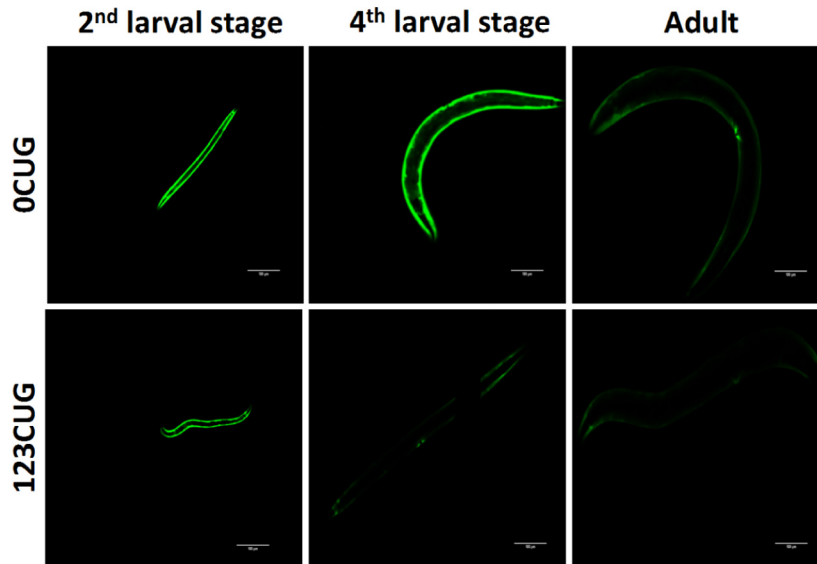
CTG- and CAG-bearing genes are affected by expanded CUG repeat expression

If the CUG repeats are processed and serve as small non-coding RNAs, we expect that they will have an effect on gene expression. We predict the effect to be particular to CUG repeat-bearing transcripts that would then be targeted by these repeat siRNAs. To address this, we performed transcriptome analysis by RNAseq of 2-day-old adults 123CUG and 0CUG strains and compared their gene expression levels. We identified and compared the 463 endogenous transcripts

Fig. 3. GFP fluorescence declines as animals developed into adults. (a) Fluorescent microscopy images of 123CUG and 0CUG control animals at different larval stages, L2, L4, and 3-day-old adults. The images show that at different stages the 123CUG animals exhibited different GFP signal levels, decreasing with age. Three to five independent experiments were performed (the bar represents 100 μ m). (b) 123 CUG animals show decreased GFP signal. The GFP signal was computationally quantified using ImageJ software for 20 animals of each 0CUG and 123CUG in 3-day-old adults. (**** $P < 0.0001$).

(a)

GFP fluorescence declines as animals develop



(b)

123 CUG animals show decreased GFP signal

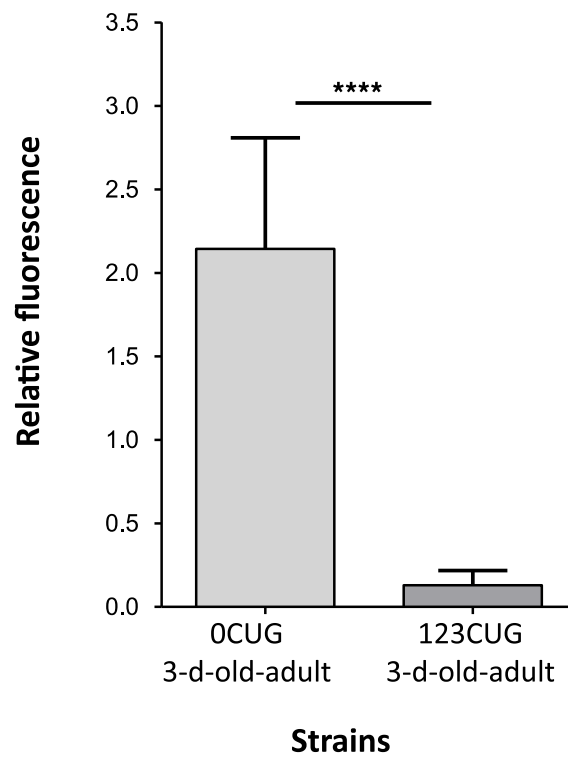


Fig. 3 (legend on previous page)

Table 1. Effect of knocking-down members of the RNAi machinery on GFP levels in 123CUG animals

Gene	GFP	Gene	GFP
<i>ain-1</i>	+	<i>ain-2</i>	-
<i>alg-2</i>	+	<i>alg-1</i>	-
<i>alg-4</i>	+	<i>cgh-1</i>	-
<i>cid-1</i>	+	<i>csr-1</i>	-
<i>drh-3</i>	+	<i>dcr-1</i>	-
<i>drsh-1</i>	+	<i>drh-1</i>	-
<i>eri-9</i>	+	<i>ego-1</i>	-
<i>mut-14</i>	+	<i>ekl-1</i>	-
<i>mut-15</i>	+	<i>ergo-1</i>	-
<i>mut-16</i>	+	<i>eri-1</i>	-
<i>mut-2</i>	+	<i>eri-3</i>	-
<i>nhl-2</i>	+	<i>eri-6</i>	-
<i>nrde-3</i>	+	<i>eri-7</i>	-
<i>pir-1</i>	+	<i>pash-1</i>	-
<i>rde-2</i>	+	<i>ppw-1</i>	-
<i>rde-4</i>	+	<i>pup-2</i>	-
<i>rsd-6</i>	+	<i>rde-1</i>	-
<i>sago-2</i>	+	<i>rsd-3</i>	-
<i>tsn-1</i>	+	<i>sago-1</i>	-
<i>vig-1</i>	+	<i>sid-1</i>	-
<i>xrn-2</i>	+	<i>sid-2</i>	-
<i>xpo-1</i>	+	<i>wago-2</i>	-
<i>wago-4</i>	-	ZK757.2	-
<i>ncbp-2</i>	Lethal	<i>mut-7</i>	Lethal
<i>lin-41</i>	Lethal	<i>ncbp-1</i>	Lethal

Quantification of images as in Fig. S1. (+) indicates greater fluorescence as compared to 123CUG animals grown on EV bacteria at L4 + 3.

containing at least 4CTG or 4CUG repeats. These transcripts should comprise the potential targets for the non-coding RNAi processed from the expanded CUGs. We observed that the endogenous genes bearing at least four CTG/CAG repeats showed a small but extremely significant decrease in transcript expression in 123CUG as compared to 0CUG animals, with an expression difference of 1.6-fold ($P = 2.2 \times 10^{-16}$) (Fig. 4a and b). Our data support a model in which expanded transcripts bearing CUG repeats trigger RNA-induced silencing with downregulation of endogenous CAG/CUG-bearing transcripts. Although in a low-level manner, the effects seem progressive. Thus, we predicted that the cumulative effect of this process has the potential to be toxic over time.

As our repeats are expressed under a muscle-specific promoter, we expected that the effect of the CUG repeats would be largely limited to muscle-specific genes (i.e., genes that are not expressed in muscles would not be significantly affected). Nevertheless, for technical reasons, we performed RNA-seq using whole organisms as samples, which might have masked some of our results. We analyzed all tissues but expected to observe a more pronounced effect on the expression of muscle-specific genes. In order to test this, we examined the tissue-specific transcript downregulations in our samples using the recently published transcriptomic analysis of *C. elegans*-specific tissues [23]. The published

data include annotations of tissue-enriched genes that are both highly and differentially expressed in the neurons, muscles, hypodermis, and intestine.

We identified 982 genes that were downregulated at least 1.5-fold in 123CUG animals as compared to 0CUG in our RNA-seq and tested the overlap with the tissue-specific genes. There were 427 genes specifically expressed in muscle and almost 25% (94 genes) of these were downregulated ($P < 10^{-36}$) in 123CUG animals. We also analyzed the overlap with other tissue specific genes. Out of the 867 neuron-specific genes, 14% were downregulated in the 123CUG animals, 11% were hypodermis-specific, and 17% were intestinal-specific genes (Fig. 4c). The effect on genes that were specifically expressed in nearby tissues is likely the result of non-cell-autonomous RNA silencing [24]. Small RNA trafficking to neighboring and even distant cells will dilute the silencing effect, as seen in our data.

Next, we checked the *C. elegans* transcripts with the longest stretch of endogenous repeats, as these were the most obvious targets for siRNA silencing. We BLAST searched the *C. elegans* genome for genes with seven or more CTG/CAG repeats and with no more than two mismatches (e -value < 0.003). We identified 31 transcripts with long endogenous repeats. We collected RNA from 1-day-old adult 123CUG and 0CUG animals and analyzed the expression levels of 24 of these genes by ddPCR. We were unable to generate specific primers and establish expression levels for the seven remaining genes. Twenty-three of 24 genes analyzed by ddPCR showed a lower expression in 123CUG animals (Fig. 5a) relative to the levels seen in 0CUG controls. Table 1S presents the human orthologs together with a general description of these genes.

Feeding wild-type *C. elegans* (N2) with *Escherichia coli* expressing a plasmid expressing CTG repeats is a direct way to activate the RNAi pathway and investigate its effects. We fed wild-type animals bacteria expressing 50 CTG repeats and analyzed gene expression in one-day-old adults for the same 24 genes tested in the 123CUG strain. Twenty-two genes were downregulated in 50CTG RNAi-treated worms (Fig. 5b). These results suggest that the dsRNA generated from 50CTG RNAi can target and silence endogenous genes with complementary repeats.

RNAi genes affect DM1 disease phenotypes in *C. elegans*

To examine whether components of the RNAi machinery affect disease phenotypes that are associated with expansion repeats, we tested 19 genes that comprise the RNAi machinery and that were positive on the GFP screen (Table 1). We examined their effect on the 123CUG's sensitivity to high temperature (34 °C) and impaired motility.

123CUG and 0CUG animals were grown for two generations on control or RNAi bacteria of each specific

gene until day 1 of adulthood. Sixty adult animals were then transferred onto empty plates, incubated at 34 °C for 21 h, and their rates of survival were scored every 2 h. As shown in Fig. 6, knocking down five positive genes, *alg-4*, *nhl-2*, *drh-3*, *alg-2*, and *mut-14*, had a protective effect on the sensitivity to high-temperature conditions. While the 0CUG animals were barely affected by downregulation of the genes tested, a clear increase in survival rates was observed for 123CUG animals grown on RNAi target genes versus the same strain grown on control bacteria (Fig. 6).

In addition to susceptibility to heat shock, 123CUG's motility impairment phenotype was also analyzed to identify the contribution of the RNAi machinery to pathogenesis caused by RNA repeats. In this case, 20 genes identified as positive from the GFP screen were tested for their effect on 123CUG's impaired motility. 123CUG and 0CUG animals were fed bacteria that express target RNAi or control bacteria, and rates of motility were recorded and analyzed using Tracker software [19]; we tested 20 animals for each condition. Downregulation of 15 genes significantly improved 123CUG motility (Fig. 7) as compared to the animals that were fed with EV bacteria. Conversely, there were no changes in the motility of 0CUG that were fed with bacteria that express RNAi toward the same genes (Fig. 2S).

Altering the RNAi machinery rescues the reduction of gene expression for genes containing seven CUG repeats or more

To investigate the rescue effect of knocking down components of the RNAi machinery in 123CUG animals, we performed qPCR to measure the expression levels of genes containing seven CUG repeats or more on 123CUG and 0CUG animals whose RNAi components were downregulated. In Fig. 5, we observed a reduction in RNA levels for 23 repeat-containing genes in wt strains that were treated with 50CTG RNAi as well as 123CUG animals. These data, together with the rescue of the motility and heat shock phenotypes (Figs. 6 and 7), led us to hypothesize that downregulation of the RNAi machinery should lead to an upregulation of the genes targeted by the non-specific siRNAs. 123CUG animals were grown on *drh-3*, *mut-14*, *alg-4*, and EV RNAi for two generations. Control groups of 0CUG animals were also treated with RNAi for each of the genes. RNA was extracted from worms at their first day of adulthood, and gene expression levels were analyzed by qPCR. As depicted in Fig. 8, downregulation of RNAi machinery components rescues the off-target silencing of endogenous transcripts previously observed in 123CUG animals.

The control group of 0CUG animals treated with RNAi was analyzed in comparison to 0CUG animals fed EV in order to ensure that the effect was related to the CUG repeats. Twenty-three of 24 genes showed no significant difference in comparison to the control group

(see Table 2S). This observation validates the conclusion that the expression of expanded CUG "stretches" leads to RNAi-mediated knockdown of endogenous genes that bear these repeats.

Discussion

DM1 is a hereditary disease that results from an expansion of CUG repeats in the 3' UTR of the DMPK gene. A key question is how the untranslated repeat RNAs acquire a toxic function and lead to the development of the disease. One of the most recent hypotheses suggests the involvement of the RNAi pathway in the toxic mechanism that underlies DM1 [25–27].

Our *C. elegans* DM1 model, expressing CUG expanded repeats in body-wall muscle cells, is a powerful, fast, and easy-to-handle system to study RNA repeat toxicity. In contrast to the slow development of the disease's pathophysiology in humans, the short life span of *C. elegans* can dramatically accelerate RNA toxicity research from years to days [4]. Furthermore, mammals and *C. elegans* show a high degree of gene and cellular pathway conservation. Research using *C. elegans* has led to many breakthroughs toward understanding human traits such as polycystic kidney disease [28], ciliopathies [29], and programmed cell death, and, most relevant to this work, the discovery of RNAi [30], microRNAs [31,32], and their connections to splicing [21].

In this study, we showed that expanded CUG repeats affect *C. elegans* in ways analogous to human DM1 symptoms. In addition, we showed that *C. elegans* fed bacteria that express dsRNA bearing CTG repeats, as a direct way of activating the RNAi machinery, exhibited a phenotype comparable, although weaker, to 123CUG (DM1) animals, supporting the roles of these pathways in DM dysfunction. We predict that the difference in phenotypic severity between RNAi feeding and the 123CUG strain is likely due to three main factors: a weaker effect of the RNAi by feeding [33] as compared to the strong RNA repeat expression in DM1 animals, the shorter length of the repeats (50CTGs), and the fact that RNAi dysregulation represents only one of several factors that contribute to CUG repeat toxicity, in these complex disorders.

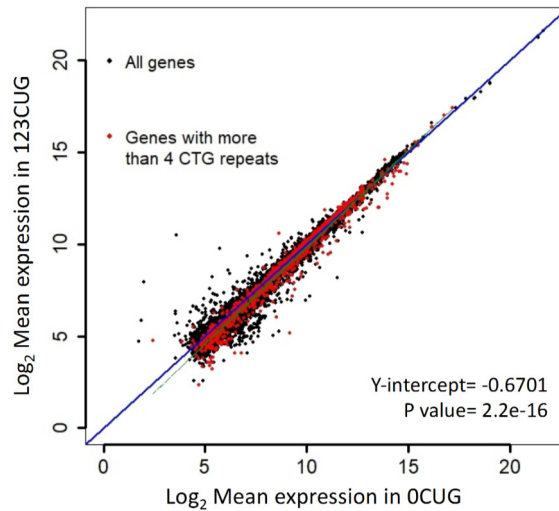
The expected effect of CUG repeats as templates for the RNA machinery would be a moderate silencing of a wide range of endogenous targeted genes. Importantly, our study showed that 23 out of the 24 genes with the longest endogenous repeats containing seven or more CTG/CAG repeats were downregulated in 123CUG worms relative to controls (0CUG). These results clearly support the involvement of siRNA mechanisms in DM1 pathogenesis and also highlight the potential for sustained, off-target, deleterious effects caused by dysfunctions of the siRNA pathway and the role they may represent in repeat disorders.

One limitation of our study was the tissue-specific expression of CUG repeats in the body wall muscle cells, whereas for technical reasons, we sequenced whole animals. Initially, we expected a large local

effect on gene expression in body wall muscle cells, attenuated by the presence of other tissues in the collected samples. However, unbiased analysis of the RNA sequencing data revealed disrupted genes to be

(a)

A scatter plot of \log_2 fold change in 123CUG gene expression



(b)

Density distribution plot of \log_2 expression in 123CUG compared to 0CUG

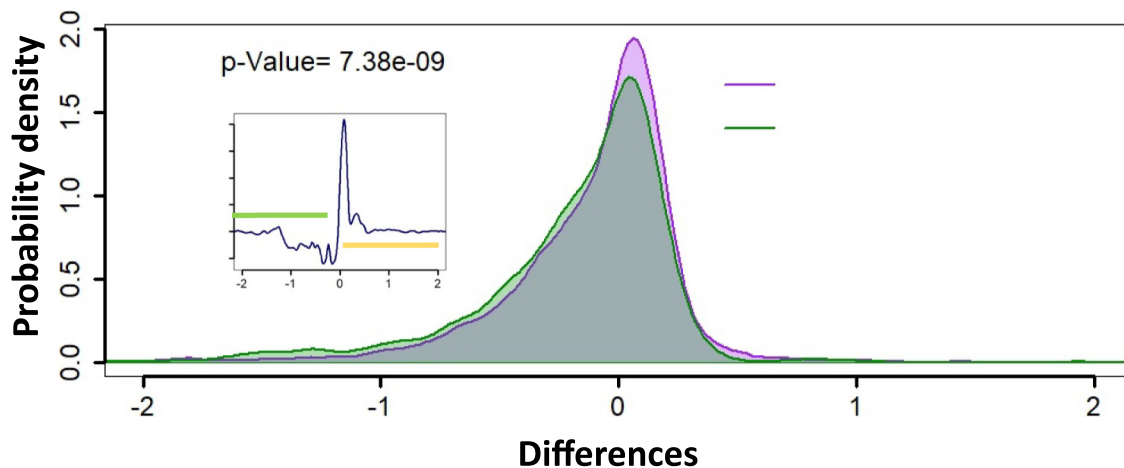


Fig. 4. RNA-seq analysis of gene expression changes in 123CUG. (a) A scatterplot of \log_2 fold change in 123CUG gene expression. Scatterplot of 123CUG as compared to 0CUG strains. In red are 463 genes bearing endogenous nucleotide repeats of four or more pure CAG/CTG repeats (e.g., CAGCAGCAGCAG or CTGCTGCTGCTG). A shift is shown in the slope of the regression line of the genes bearing repeats as compared to all genes. This shift is also evident in the density plot. (b) Density distribution plot of \log_2 expression in 123CUG compared to 0CUG. Density distribution plot of the difference in gene expression between 123CUG and the control (0CUG) strains for all genes (purple) and for the 463 genes carrying endogenous repeats (green). The overlap between the distribution is shown in gray. The left shift in the distribution shown in green indicates the increase in downregulated genes bearing repeats in 123CUG animals ($P < 7 \times 10^{-9}$, t test). The difference between the two highlighted distributions is shown in the box. (c) Tissue-expressed enrichment analyses of downregulated genes. We tested the overlap between the genes that were downregulated in 123CUG (>1.5 -fold relative to 0CUG) and the genes that expressed either in the neurons, muscle, hypodermis, and intestine, as determined by Kaletsky *et al.* [23]. These genes significantly overlapped in all the tissues ($P < 0.001$, hypergeometric test).

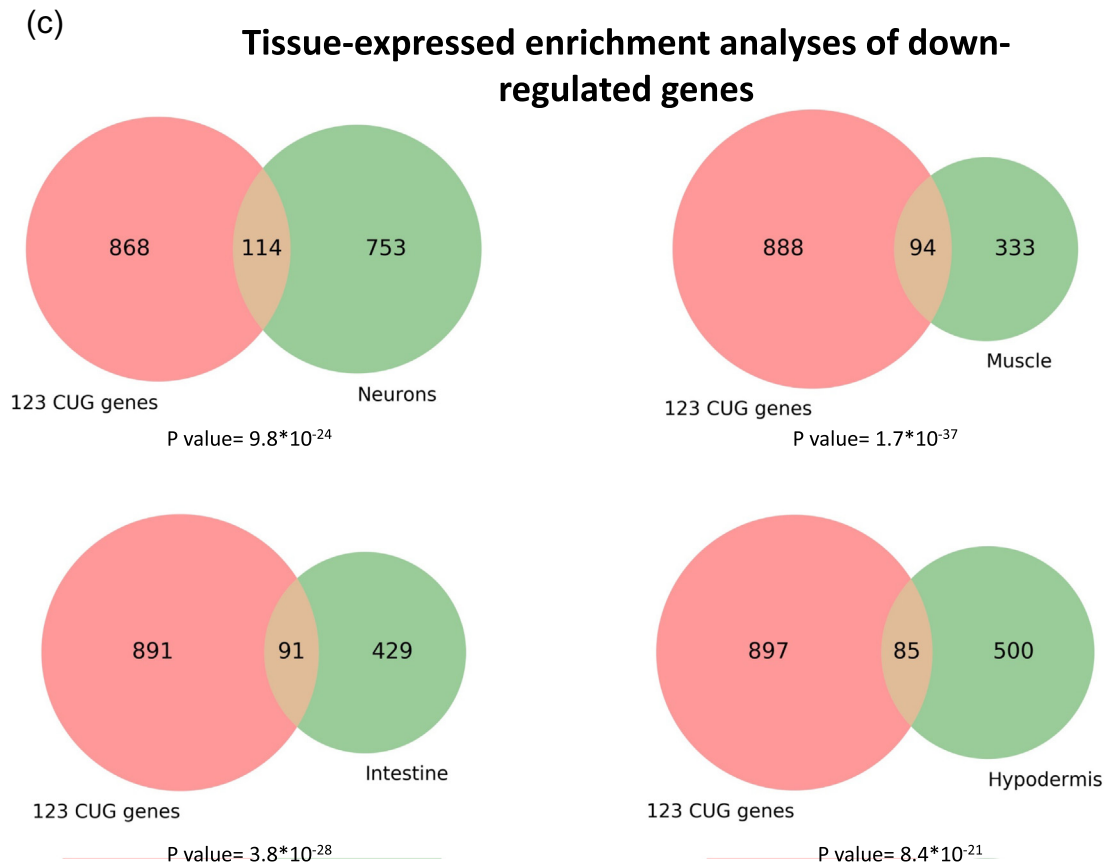


Fig. 4. (continued).

equally enriched for different tissues. Therefore, we propose that the expression changes, at least of some genes, are small and global. One possible mechanism for propagation of the silencing effect to nearby tissues is non-cell-autonomous RNA silencing.

In our experiments, the therapeutic potential of modulating the activity of the RNAi machinery manifested itself in three major modes: rescue of GFP levels, reduction of disease phenotypes (improved motility), and rescue of reduction in expression of genes containing CTG-repeats. Rescue of GFP levels (Table 1) indicates a protective role of the RNAi machinery in DM1 pathology: the machinery breaks down aberrant transcripts and prevents RNA toxicity. However, when five members (*mut-14*, *alg-4*, *drh-3*, *alg-2*, and *nhl-2*) of the small RNA pathway were knocked-down, DM1 animals showed improvement in heat sensitivity. Likewise, the motility phenotype improved when genes of small RNA pathway were knocked-down. Furthermore, we observed an upregulated expression of genes containing CTG/CAG repeats (Fig. 8) that were reduced in 123CUG animals (Fig. 5). This supports a complex role for the RNAi machinery with some beneficial effects as well as a wide range of deleterious effects. When repeat-containing transcripts

trigger potential deleterious effects, the RNAi machinery is hyper-activated and, as such, contributes to disease pathogenesis and is associated with several phenotypes.

Analysis of the human genome for genes with seven or more naturally occurring CTG/CAG repeats revealed over 600 genes. These genes have the potential to be targets for the RNAi machinery in the background of DM1 diseases and long CUG repeats. The large number of potential target genes further underscores the wide range of cellular processes susceptible to arbitrary disruption of their expression. Although in humans such effects can be extremely variable depending on the tissue, cell, and developmental conditions, our findings suggest a model in which expanded RNA accumulation and RNA foci activate RISC, which in turn randomly silences other CTG containing genes. The recent development of new sequencing methods, deep analysis of different cell types and tissues, will be essential in detecting small transcriptional changes of repeat-bearing RNAs in these tissues and in shedding light on their link to muscular and neuronal phenotypes seen in patients with trinucleotide repeat disorders.

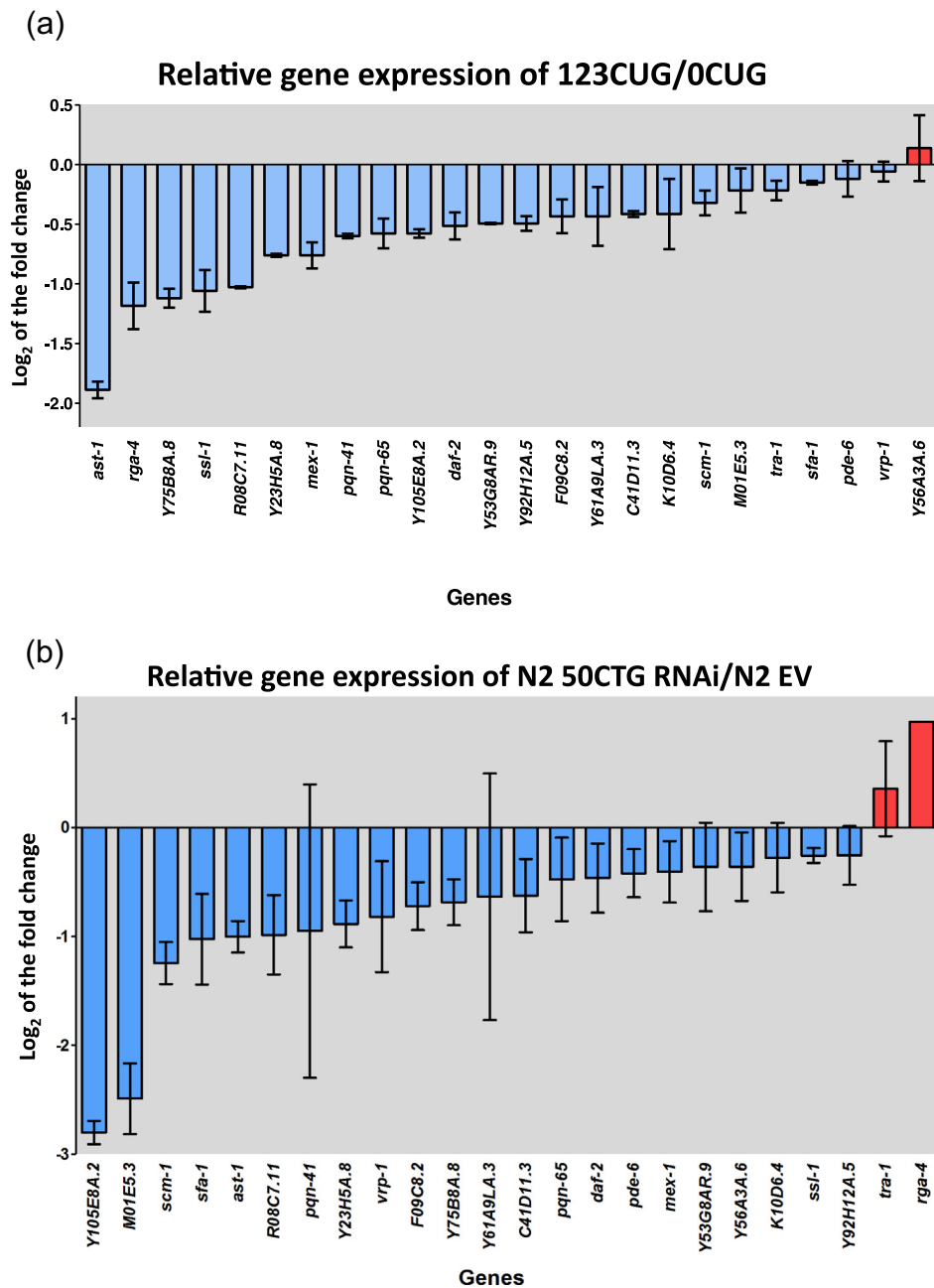


Fig. 5. ddPCR of genes containing seven repeats or more in DM1-like animals. (a) Relative gene expression of 123CUG/0CUG. RNA levels are reduced in 123CUG as compared to 0CUG, determined by ddPCR. Error bars represent the standard deviation (s.d.) from two independent, for which two technical replicates were analyzed. In these experiments, hundreds of animals were collected. (b) Relative gene expression of N2 50CTG RNAi/N2 EV. Downregulation in gene expression of wt (N2) fed 50CTG RNAi as compared to wt (N2) fed EV was determined by qPCR. Error bars represent s.d. and are the result of three biological and three technical repeats.

Our work revealed a mechanism of pathogenesis in *C. elegans* that, if relevant to humans, may shed light and explain the late onset of several repeat diseases and the correlation between repeat length and disease pathophysiology (longer repeats may correspond to more substrate to generate siRNAs). In addition, RNAi silencing and the distinct silencing of endogenous

targets due to the heterogeneity between tissues, or random events may also contribute to variability in disease progression between patients. This mechanism provides new targets for therapeutic intervention for patients with myotonic dystrophy. Finally, a similar mechanism may be relevant to other repeat-based degenerative disorders.

Materials and Methods

C. elegans and RNAi strains

C. elegans strains GR2024 (123CUG) and GR2025 (0CUG) [5] were used. These animals express 123CUG or 0CUG repeats in the 3'UTR of GFP in the body wall muscle cells under the *myo-3* promoter. The N2 (Bristol) strain was obtained from the Caenorhabditis Genetics Center (Minneapolis, USA) and used as a wild-type strain. *C. elegans* strains were handled using standard methods [34] and grown at 20 °C unless otherwise indicated.

The 50CTG dsRNA expressing bacteria was manufactured by designing 50CTG oligos and transformed it to HT115 bacteria. The chosen vector for this design is L4440. 50xCTG oligo and 50xCAG with 5xphosphate was annealed and ligated into the *EcoRV* site. Bacterial strains (*E. coli*) expressing EV (L4440) and dsRNA were used for RNAi experiments. All 49 RNAi constructs used were obtained from the Ahringer's library.

Gene inactivation

RNAi-mediated gene inactivation was achieved by feeding worms dsRNA [35], and RNAi clones used for gene inactivation were obtained from the Ahringer's library. A single colony of RNAi bacteria of the desired knockdown gene was grown overnight in 2.5 ml LB medium [10 g Bacto-tryptone, 5 g Bacto-yeast, 5 g NaCl, H₂O to 1 L (pH 7.5)] with 2 µl ampicillin, at 37 °C with shaking. One hundred milliliters of the culture was spotted in the middle of 8-ml NGM plates with carbenicillin. Vector expression was induced by adding IPTG for a final concentration of 0.5–1 mM directly over the bacterial lawn and let dry for 24 h. Empty L4440 vector (EV) was used as a negative control. Nematodes were synchronized by NaOCl bleaching and overnight hatching in M9 solution (3 g KH₂PO₄, 6 g Na₂HPO₄, 5 g NaCl, 1 ml 1 M MgSO₄, H₂O to 1 L). Twenty to 30 L1 larval stage nematodes (~24 h after synchronization) were aliquoted onto agar plates containing the 24-h culture of RNAi bacteria expressing dsRNA and allowed to develop to adulthood. The process was repeated and the second-generation worms were grown until day 1 of adulthood.

Heat shock assays

Synchronized eggs were placed on NGM plates seeded with RNAi bacteria (as indicated) and supplemented with 100 mM IPTG (4 mM final concentration). For 2-day-old adults, nematodes were synchronized by NaOCl bleaching and overnight hatching in M9 solution. Twenty to 30 L1 larval stage nematodes (~18 h after synchronization) were aliquoted onto agar plates seeded with the RNAi bacteria and allowed to develop to day 1 of adulthood. To test the worms'

susceptibility to heat stress, 60 animals were transferred onto pre-warmed plates without bacteria (10 animals per plate) and exposed to 34 °C. Survival rates were recorded every 2 h.

RNA sequencing library preparation

The 123CUG and 0CUG strains were synchronized by bleaching and plated as L1 larvae on RNAi plates seeded with HT115 bacteria carrying empty L4440 vectors. To prevent the hatching of the progeny, worms were transferred to plates containing 10 µM of 5-fluorouracil (Sigma) at the L4 stage. Worms were collected and frozen immediately in liquid nitrogen at day 2 of adulthood. Total RNA was extracted with TRIzol Reagent (Ambion) and assessed for degradation using Agilent 2100 Bioanalyzer. Three biological replicates from each strain were collected. Illumina Truseq stranded polyA-mRNA library was prepared and sequenced for 86 cycles at the DNA Sequencing and Genomics laboratory (Institute of Biotechnology, University of Helsinki). The 12 samples were multiplexed and sequenced on one lane of Illumina NextSeq 500, yielding circa 18–20 million reads per sample.

Statistical analysis

The survival analysis was performed using log-rank (Mantel-cox) and Gehan–Breslow–Wilcoxon tests, $\alpha = 0.05$. The Wilcoxon method gives more weight to deaths at early time points and does not require a consistent hazard ratio. In contrast, the log-rank test gives equal weight to all time points and is more powerful if the assumption of proportional hazards is true [36]. The log-rank test is the most common test used to compare survival curves, but both tests were used to overcome the possibility of unproportional hazards. GraphPad Prism software (USA) was used to create the graphs. The analysis for the motility assay was performed using a one-tailed Student's *t* test, $\alpha = 0.05$.

Read processing for RNA Seq data

We had ~20 million individual sequence reads for each sample. First, the quality was checked using FastQC [37]. A Trim Galore algorithm was used to apply quality and adapter trimming to FastQ files. Sequences were then compared to the WormBase WBcel235 assembly of the *C. elegans* genome using a bowtie2 algorithm [38]. There was an 83% average overall alignment rate. The number of counts for each sequence was computed using a HTSeq algorithm [39].

Identification of genes with CTG repeats in the *C. elegans* genome

We performed a BLAST search [40] for *C. elegans* genes containing four repeats of CTG/CAG.

Subsequently, this list was filtered to include only sequences that had a refseq mRNA ID. We removed replicate genes, which left a list of 436 genes. To inspect tissue enrichment in the downregulated genes, we used data on tissue-specific gene expression [23] in the neurons, muscles, hypodermis, and intestine. We assessed enrichment with the hypergeometric test.

Motility

For the motility phenotype, two assays were used. In the first assay [41], a single worm (3-day-old adult) was

placed on a fresh NGM plate seeded with a thin layer of bacteria (OP50). A 5-min movie clip was recorded using the system developed by William Schafer (<https://www.mrc-lmb.cam.ac.uk/wormtracker>). Ten worms were tested for each strain.

For the second assay [19], a full NGM plate of *C. elegans* was tested for each strain (0CUG, 123CUG, N2 EV, and N2 CUG50 RNAi) at different ages (2-, 4-, and 6-day-old adults) to test the effect of age. To test the rescuing of motility downregulation, a full NGM plate of 3-day-old adults was used with or without RNAi for both strains (0CUG and 123CUG). Images were

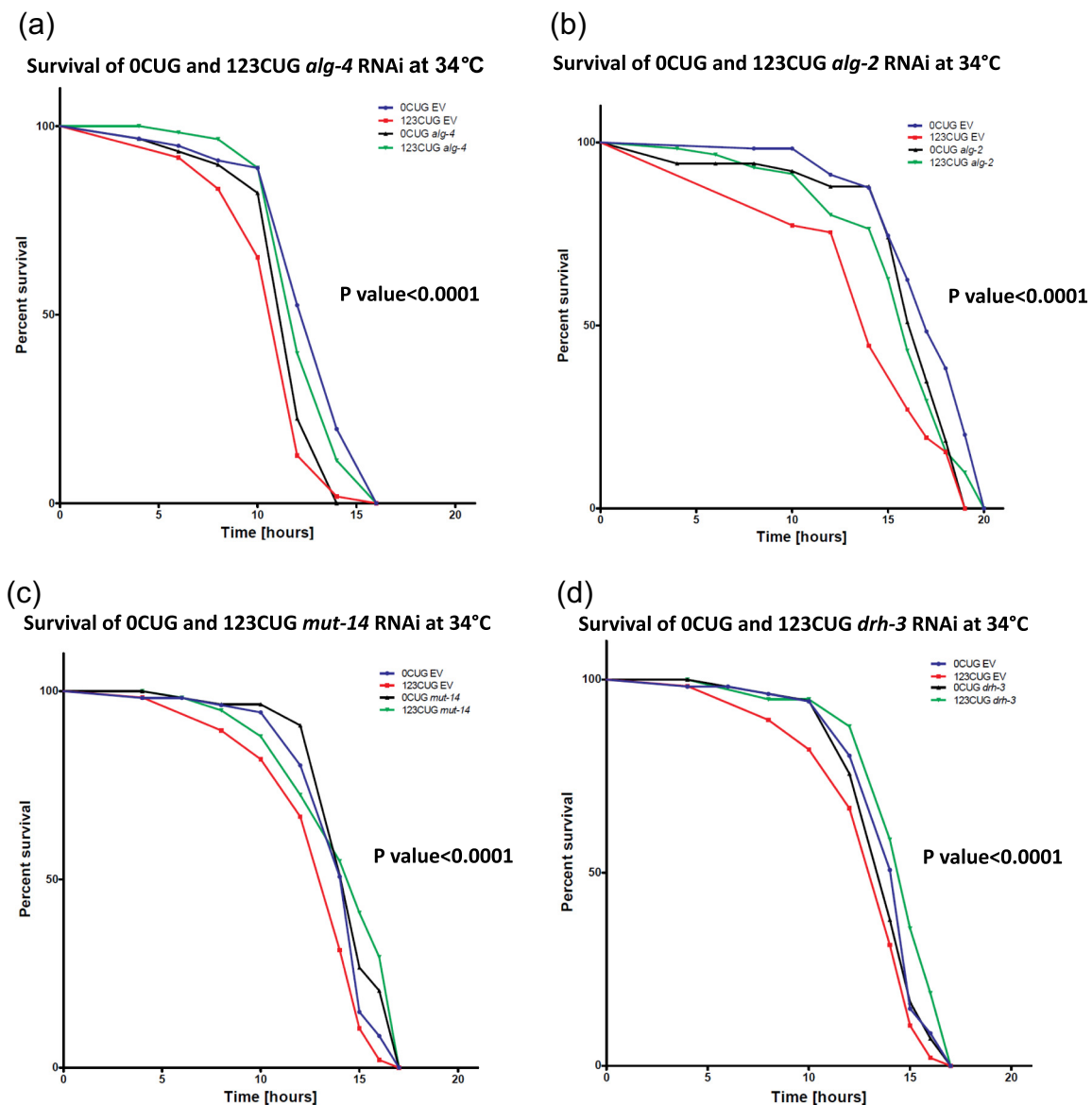


Fig. 6. Survival under heat stress is improved following RNAi machinery knockdown. Knockdown of *drh-3*, *mut-14*, *nhl-2*, *alg-2*, and *alg-4* by RNAi rescues the reduced survival under heat shock (34 °C) of 123CUG animals and does not affect the survival of 0CUG animals. The *P* value determined by log-rank and Wilcoxon tests comparing 123CUG worms grown on RNAi for different genes to 123CUG worms grown on EV was < 0.0001 in all experiments. There was no significant difference between 0CUG worms fed RNAi targeting specific genes *versus* EV. *n* = 60 for each group.

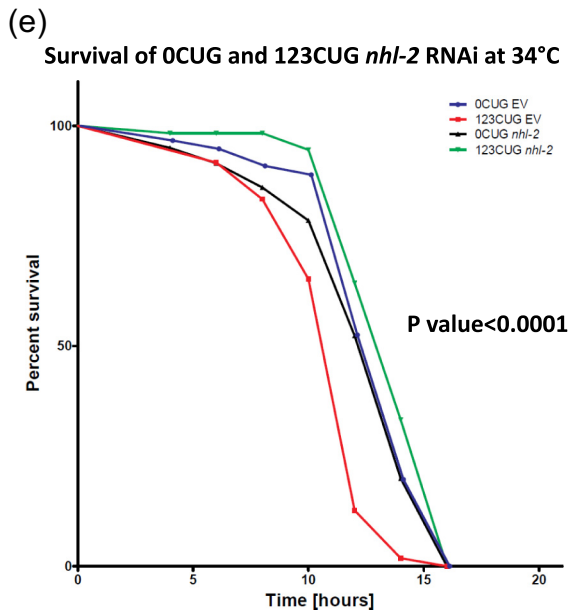


Fig. 6. (continued).

captured using a digital microscope and the Micam 20 Software. The resolution was 2048 × 1536 pixels, and a total number of 120 frames were taken at a rate of 1

capture per second for 120 s. All images were captured with the same focus, on the same day, at room temperature. The video was built by MakeAVi software with a playback rate of 15 frames per second. The animals were analyzed using Tracker 5.0 software by defining the head of the animal as a point mass and manually tracking its position for each frame.

Gene expression (ddPCR and qPCR)

Total RNA was extracted from the whole body of 2-day-old adult *C. elegans* worms using Trizol Reagent (Ambion, USA) and a NucleoSpin RNA isolation kit (Macherey-Nagel, Germany). Reverse transcription was performed using a cDNA reverse transcription kit (Applied Biosystems, USA), and mRNA expression levels were measured with qPCR and digital-droplet PCR. For qPCR, SYBR-Green (Bio-Rad, USA) was used in a CFX-384 Real-Time PCR system (Bio-Rad). Data were analyzed using the $\Delta\Delta C_t$ method. For digital-droplet PCR, the mRNA expression was measured by using a QX200 Bio-Rad digital droplet PCR system. Relative quantities of gene transcripts in both assays were normalized to *rpl-32* and *cdc-42*. All the primers (Table 3S) used in this research were designed using the NCBI Primer Blast and checked by Hylabs.

Motility improvement following RNAi machinery knockdown

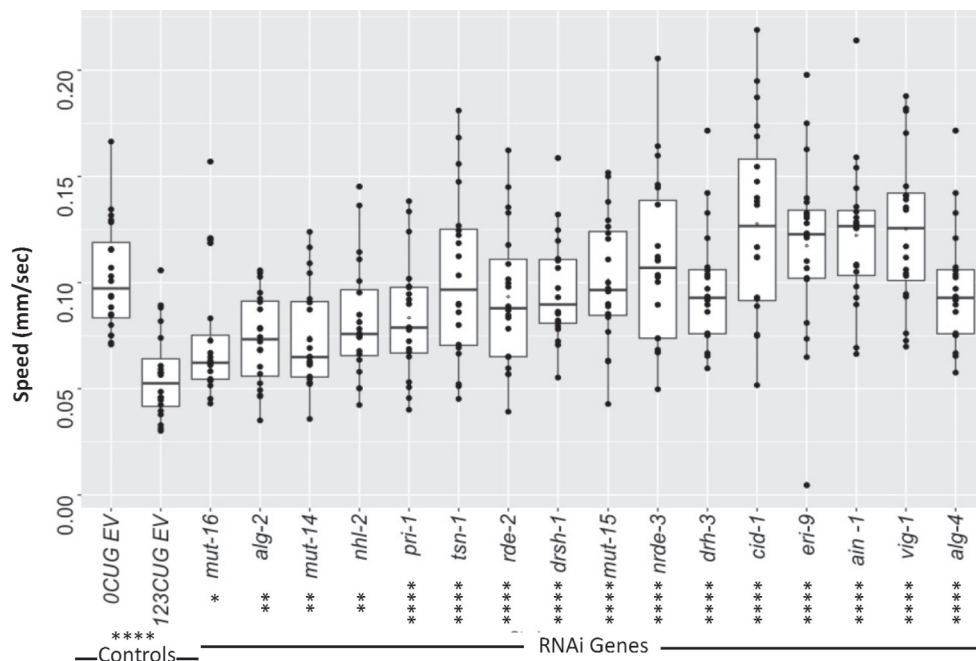


Fig. 7. Motility following RNAi machinery knockdown. Plotted data correspond to the speed of 3-day-old adults 123CUG fed RNAi targeting RNAi genes. Fifteen genes cause a significant improvement in the speed of 123CUG following RNAi knockdown as compared to 0CUG. No effect was observed for 0CUG when RNAi components were downregulated as compared to 0CUG EV (see Fig. 2S). Two independent experiments were carried out; in each experiment, 10 animals were analyzed for each strain at room temperature, with *P* values determined by a one-tailed Student's *t* test (**P* < 0.05, ***P* < 0.01, *****P* < 0.0001).

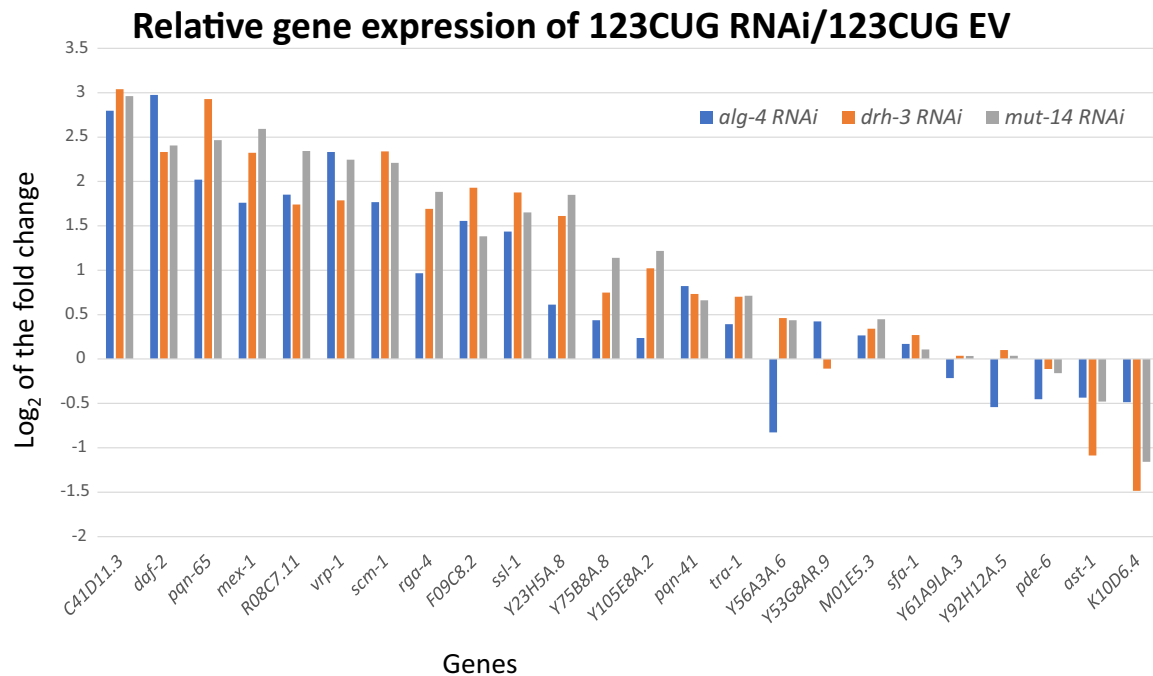


Fig. 8. qPCR of genes containing seven repeats or more in 123CUG animals who underwent knockdown of RNAi machinery components. A fold change in gene expression of 123CUG animals whose siRNA components were downregulated relative to 123CUG animals fed EV. Results are normalized to the 0CUG control strain. The majority of the genes analyzed by qPCR exhibited a rescue effect as they were overexpressed relative to 123CUG animals grown on EV (see Fig. 5). Technical replicates were analyzed for this experiment.

Imaging and signal quantification

The 123CUG and 0CUG strains were grown for two generations on EV bacteria or on RNAi bacteria (49 genes). For *nhl-2*, *mut-14*, *drh-2*, and *alg-4*, images were taken at three different ages (L2, L4, 2-day-old adults). The rest of the RNAi strains were imaged at 2-day-old adults. The worms were washed twice with M9, anesthetized using 15 mM sodium azide (Sigma, #S-2002), and placed on an agar pad. Images were taken using a Nikon C2 confocal microscope. Quantitative fluorescence analyses were performed using ImageJ software (<https://imagej.net/Welcome>).

Supplementary data to this article can be found online at <https://doi.org/10.1016/j.jmb.2019.03.003>.

Acknowledgements

We would like to thank the BIRAX, the Institute for Medical Research Israel-Canada and the Academy of Finland for their generous support to our project. Orion foundation for the prusiner-abramsky research award. We would also like to thank Dr. Julie M. Claycomb at the Department of Molecular Genetics, University of Toronto and her research group, especially Dr. Monica

Wu and Uri Seroussi, for their insight on small RNA pathways and their expertise with IP techniques. Prof. Millet Treinin at the Department of Medical Neurobiology, Hebrew University -Hadassah Medical School for her assistance and support, as well as Ayman Qawasmi and Nitzan Guberman for their help in graphical abstract design and assistance in the GFP fluorescence analysis respectively.

Received 1 November 2018;

Received in revised form 28 February 2019;

Accepted 7 March 2019

Available online 14 March 2019

Keywords:

RNA toxicity;
RNA interference;
myotonic dystrophy;
C. elegans;
trinucleotide repeat disorders

†Lena Qawasmi & Maya Braun these authors contributed equally to this work.

Abbreviations used:

DM1 and DM2, myotonic dystrophy types 1 and 2; 3'UTR, 3' untranslated region; dsRNA, double-stranded RNA;

RNAi, RNA interference; MBNL1, muscleblind-like 1; GFP, green fluorescent protein; EV, empty vector.

References

- [1] R.I. Richards, Dynamic mutations: a decade of unstable expanded repeats in human genetic disease, *Hum. Mol. Genet.* 10 (2001) 2187–2194.
- [2] D.L.B.E. Kasper, S. Hauser, D. Longo, J.L. Jameson, A.S. Fauci, Harrison's Principles of Internal Medicine, 16th, 1, 2005, 2530.
- [3] C. Turner, D. Hilton-Jones, The myotonic dystrophies: diagnosis and management, *J. Neurol. Neurosurg. Psychiatry* 81 (2010) 358–367.
- [4] S.M. Garcia, Y. Tabach, G.F. Lourenco, M. Armakola, G. Ruvkun, Identification of genes in toxicity pathways of trinucleotide-repeat RNA in *C. elegans*, *Nat. Struct. Mol. Biol.* 21 (2014) 712–720.
- [5] A.F. Klein, E. Gasnier, D. Furling, Gain of RNA function in pathological cases: focus on myotonic dystrophy, *Biochimie* 93 (2011) 2006–2012.
- [6] J.W. Miller, C.R. Urbinati, P. Teng-Umnuay, M.G. Stenberg, B.J. Byrne, C.A. Thornton, et al., Recruitment of human muscleblind proteins to (CUG)(n) expansions associated with myotonic dystrophy, *EMBO J.* 19 (2000) 4439–4448.
- [7] T. Zu, B. Gibbens, N.S. Doty, M. Gomes-Pereira, A. Huguet, M.D. Stone, et al., Non-ATG-initiated translation directed by microsatellite expansions, *Proc. Natl. Acad. Sci. U. S. A.* 108 (2011) 260–265.
- [8] J.M. Fernandez-Costa, A. Garcia-Lopez, S. Zuniga, V. Fernandez-Pedrosa, A. Felipo-Benavent, M. Mata, et al., Expanded CTG repeats trigger miRNA alterations in *Drosophila* that are conserved in myotonic dystrophy type 1 patients, *Hum. Mol. Genet.* 22 (2013) 704–716.
- [9] A. Bansal, L.J. Zhu, K. Yen, H.A. Tissenbaum, Uncoupling lifespan and healthspan in *Caenorhabditis elegans* longevity mutants, *Proc. Natl. Acad. Sci. U. S. A.* 112 (2015) E277–E286.
- [10] R. Perbellini, S. Greco, G. Sarra-Ferraris, R. Cardani, M.C. Capogrossi, G. Meola, et al., Dysregulation and cellular mislocalization of specific miRNAs in myotonic dystrophy type 1, *Neuromuscul. Disord.* 21 (2011) 81–88.
- [11] G. Sicot, M. Gomes-Pereira, RNA toxicity in human disease and animal models: from the uncovering of a new mechanism to the development of promising therapies, *Biochim. Biophys. Acta* 1832 (2013) 1390–1409.
- [12] T.A.W.L. Cooper, G. Dreyfuss, RNA and Disease, *Cell.* 136 (4) (2009) 777–793.
- [13] H. Du, M.S. Cline, R.J. Osborne, D.L. Tuttle, T.A. Clark, J.P. Donohue, et al., Aberrant alternative splicing and extracellular matrix gene expression in mouse models of myotonic dystrophy, *Nat. Struct. Mol. Biol.* 17 (2010) 187–193.
- [14] R.J. Osborne, X. Lin, S. Welle, K. Sobczak, J.R. O'Rourke, M. S. Swanson, et al., Transcriptional and post-transcriptional impact of toxic RNA in myotonic dystrophy, *Hum. Mol. Genet.* 18 (2009) 1471–1481.
- [15] A. Mykowska, K. Sobczak, M. Wojciechowska, P. Kozlowski, W.J. Krzyzosiak, CAG repeats mimic CUG repeats in the misregulation of alternative splicing, *Nucleic Acids Res.* 39 (2011) 8938–8951.
- [16] J. Krol, A. Fiszler, A. Mykowska, K. Sobczak, M. de Mezer, W. J. Krzyzosiak, Ribonuclease dicer cleaves triplet repeat hairpins into shorter repeats that silence specific targets, *Mol. Cell* 25 (2007) 575–586.
- [17] M.S. Song, J.J. Rossi, Molecular mechanisms of Dicer: endonuclease and enzymatic activity, *Biochem. J.* 474 (2017) 1603–1618.
- [18] N. Zhang, T. Ashizawa, RNA toxicity and foci formation in microsatellite expansion diseases, *Curr. Opin. Genet. Dev.* 44 (2017) 17–29.
- [19] M. Wojciechowska, W.J. Krzyzosiak, Cellular toxicity of expanded RNA repeats: focus on RNA foci, *Hum. Mol. Genet.* 20 (2011) 3811–3821.
- [20] M.G. Santoro, Heat Shock Factors and the Control of the Stress Response, 59, Elsevier Science, 2000 55–63.
- [21] Y. Tabach, A.C. Billi, G.D. Hayes, M.A. Newman, O. Zuk, H. Gabel, et al., Identification of small RNA pathway genes using patterns of phylogenetic conservation and divergence, *Nature.* 493 (2013) 694–698.
- [22] J.K. Kim, H.W. Gabel, R.S. Kamath, M. Tewari, A. Pasquinelli, J. F. Rual, et al., Functional genomic analysis of RNA interference in *C. elegans*, *Science.* 308 (2005) 1164–1167.
- [23] R. Kaletsky, V. Yao, A. Williams, A.M. Runnels, A. Tadych, S. Zhou, et al., Transcriptome analysis of adult *Caenorhabditis elegans* cells reveals tissue-specific gene and isoform expression, *PLoS Genet.* 14 (2018), e1007559.
- [24] O. Voynet, Non-cell autonomous RNA silencing, *FEBS Lett.* 579 (2005) 5858–5871.
- [25] E. Marti, X. Estivill, Small non-coding RNAs add complexity to the RNA pathogenic mechanisms in trinucleotide repeat expansion diseases, *Front. Mol. Neurosci.* 6 (2013) 45.
- [26] M. Banez-Coronel, S. Porta, B. Kagerbauer, E. Mateu-Huertas, L. Pantano, I. Ferrer, et al., A pathogenic mechanism in Huntington's disease involves small CAG-repeated RNAs with neurotoxic activity, *PLoS Genet.* 8 (2012), e1002481.
- [27] J.R. Gatchel, H.Y. Zoghbi, Diseases of unstable repeat expansion: mechanisms and common principles, *Nat. Rev. Genet.* 6 (2005) 743–755.
- [28] M.M. Barr, P.W. Sternberg, A polycystic kidney-disease gene homologue required for male mating behaviour in *C. elegans*, *Nature.* 401 (1999) 386–389.
- [29] M.M. Barr, *Caenorhabditis elegans* as a model to study renal development and disease: sexy cilia, *J. Am. Soc. Nephrol.* 16 (2005) 305–312.
- [30] A. Fire, S. Xu, M.K. Montgomery, S.A. Kostas, S.E. Driver, C. C. Mello, Potent and specific genetic interference by double-stranded RNA in *Caenorhabditis elegans*, *Nature.* 391 (1998) 806–811.
- [31] B.J. Reinhart, F.J. Slack, M. Basson, A.E. Pasquinelli, J.C. Bettinger, A.E. Rougvie, et al., The 21-nucleotide let-7 RNA regulates developmental timing in *Caenorhabditis elegans*, *Nature.* 403 (2000) 901–906.
- [32] R.C. Lee, R.L. Feinbaum, V. Ambros, The *C. elegans* heterochronic gene lin-4 encodes small RNAs with antisense complementarity to lin-14, *Cell.* 75 (1993) 843–854.
- [33] L.F.A. Timmons, Specific interference by ingested dsRNA, *Nature* 359 (1998) 854.
- [34] S. Brenner, The genetics of *Caenorhabditis elegans*, *Genetics.* 77 (1974) 71–94.
- [35] R.S. Kamath, M. Martinez-Campos, P. Zipperlen, A.G. Fraser, J. Ahringer, Effectiveness of specific RNA-mediated interference through ingested double-stranded RNA in *Caenorhabditis elegans*, *Genome Biol.* 2 (2001) (RESEARCH0002).
- [36] H.F.J. Jiang, Survival analysis, *Methods in Molecular Biology* (Clifton, NJ), 404, 2007.

-
- [37] S. Andrews, FastQC: A Quality Control Tool for High Throughput Sequence Data, 2010.
- [38] B. Langmead, S.L. Salzberg, Fast gapped-read alignment with Bowtie 2, *Nat. Methods* 9 (2012) 357–359.
- [39] S. Anders, P.T. Pyl, W. Huber, HTSeq—a Python framework to work with high-throughput sequencing data, *Bioinformatics* 31 (2015) 166–169.
- [40] S.F. Altschul, T.L. Madden, A.A. Schaffer, J. Zhang, Z. Zhang, W. Miller, et al., Gapped BLAST and PSI-BLAST: a new generation of protein database search programs, *Nucleic Acids Res.* 25 (1997) 3389–3402.
- [41] E. Cohen, E. Yemini, W. Schafer, D.G. Feitelson, M. Treinin, Locomotion analysis identifies roles of mechanosensory neurons in governing locomotion dynamics of *C. elegans*, *J. Exp. Biol.* 215 (2012) 3639–3648.